Angewandte International Edition Chemie

Pigments

International Edition: DOI: 10.1002/anie.201505840
German Edition: DOI: 10.1002/ange.201505840

Evidence for Degradation of the Chrome Yellows in Van Gogh's *Sunflowers*: A Study Using Noninvasive In Situ Methods and Synchrotron-Radiation-Based X-ray Techniques

Letizia Monico, Koen Janssens, Ella Hendriks, Frederik Vanmeert, Geert Van der Snickt, Marine Cotte, Gerald Falkenberg, Brunetto Giovanni Brunetti, and Costanza Miliani*

Abstract: *This paper presents firm evidence for the chemical alteration of chrome yellow pigments in Van Gogh's Sunflowers (Van Gogh Museum, Amsterdam). Noninvasive in situ spectroscopic analysis at several spots on the painting, combined with synchrotron-radiation-based X-ray investigations of two microsamples, revealed the presence of different types of chrome yellow used by Van Gogh, including the lightfast $PbCrO_4$ and the sulfur-rich $PbCr_{1-x}S_xO_4$ ($x \approx 0.5$) variety that is known for its high propensity to undergo photoinduced reduction. The products of this degradation process, i.e., Cr^{III} compounds, were found at the interface between the paint and the varnish. Selected locations of the painting with the highest risk of color modification by chemical deterioration of chrome yellow are identified, thus calling for careful monitoring in the future.*

The *Sunflowers* series, painted by Van Gogh in Arles in 1888–1889, comprises seven paintings, all depicting a bouquet of sunflowers in an earthenware pot.[1a,2] In the fourth version of the series, painted on August 23rd–24th 1888,[1a] Van Gogh replaced the blue background of the earlier compositions with a yellow one, experimenting with combinations of different yellow hues. Besides this version, which is currently at the National Gallery in London, the artist went on to make two copies of it. The first (unsigned) copy is now at the Seiji Togo Memorial Sompo Japan Nipponkoa Museum of Art (Tokyo) and the second (signed) copy, now belongs to the collection of the Van Gogh Museum (Amsterdam).[3]

The vibrancy of these artworks was made possible by the use of chrome yellows (CYs), a pigment class invented early in the 19th century with brilliant hues ranging from lemon-yellow to orange-yellow.[4,5] The chrome yellow varieties that are mentioned in a series of Van Gogh's letters of the period 1888–1890 are the chrome yellow type 1, 2, and 3, which likely correspond to the "lemon", "yellow", and "orange" tones.[1b] Despite their strong similarities, the three paintings feature different yellow tonalities with subtle variations in contrast between the sunflower petals, the background, and the table area. Comparative technical examination of the *Sunflowers* series has revealed how Van Gogh skillfully manipulated the mixing of pigments, layering, and application of paint to achieve these different effects, as he usually did when making repetitions of his works.[6,7] However, the extent to which subsequent, unintended effects of color change also play a role in the way the paintings look today has been questioned.[2,3]

Our previous studies proved that CYs (denoted as $PbCr_{1-x}S_xO_4$, with $0 \leq x \leq 0.8$, in view of the variable sulfate content) are prone to darkening because of photoreduction of the original chromate ions to Cr^{III} compounds and that Cr^{V} intermediates are thermally formed through the interaction with the oil binder. The formation of reduced Cr is favored for sulfate-rich, lemon-yellow, orthorhombic $PbCr_{1-x}S_xO_4$ varieties of the pigment (with $x > 0.4$) than for the orange-yellow, monoclinic $PbCrO_4$ that is the most lightfast of these materials.[8–12]

The aim of this study was to assess the extent to which the *Sunflowers* version owned by the Van Gogh Museum (Figure 1A) contains lightfast $PbCrO_4$ (henceforth denoted as LF-CY) and light-sensitive sulfur-rich $PbCr_{1-x}S_xO_4$ ($x > 0.4$) (LS-CY), as well as to determine whether or not these pigments have been subject to a reduction process.

Noninvasive in situ investigations, comprising macroscopic X-ray fluorescence scanning (MA-XRF),[13] and portable reflection mid-FTIR and Raman spectroscopies[14] were used to characterize the molecular composition and structure of the different CY types and their association with other pigments throughout the painting. In addition, two paint microsamples (see Figure 1A for the sampling spots), out of the nine already available, were selected for additional studies by synchrotron radiation (SR) based μ-XRD, μ-FTIR, and μ-Raman studies to retrieve information about the spatial distribution of CYs, and by SR micro X-ray absorption near

[*] Dr. L. Monico, Prof. B. G. Brunetti, Dr. C. Miliani
CNR-ISTM and SMAArt Centre
Department of Chemistry, Biology and Biotechnologies
University of Perugia
via Elce di Sotto 8, 06123 Perugia (Italy)
E-mail: letizia.monico@istm.cnr.it
Dr. L. Monico, Prof. K. Janssens, F. Vanmeert, Dr. G. Van der Snickt
Department of Chemistry, University of Antwerp
Groenenborgerlaan 171, 2020 Antwerp (Belgium)
Dr. E. Hendriks
Conservation Department, Van Gogh Museum
Paulus Potterstraat 7, 1070 AJ Amsterdam (The Netherlands)
Dr. M. Cotte
ESRF, Avenue des Martyrs 71, 38000 Grenoble (France)
and
LAMS, CNRS UMR 8220, Sorbonne Universités
UPMC Univ Paris 06, place Jussieu 4, 75005 Paris (France)
Dr. G. Falkenberg
DESY, Notkestrasse 85, 22607 Hamburg (Germany)

Supporting information for this article is available on the WWW under http://dx.doi.org/10.1002/anie.201505840.

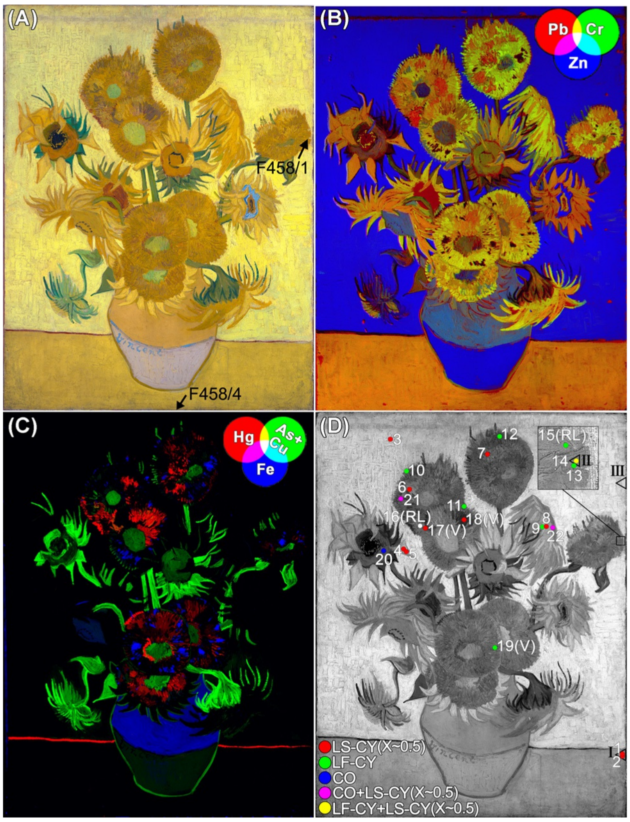

Figure 1. A) Photograph of *Sunflowers* by Van Gogh (Arles, 1889; Van Gogh Museum, Amsterdam); sampling spots are also shown. RGB composite MA-XRF maps of B) Pb/Cr/Zn and C) Hg/As + Cu/Fe. D) Raman distribution of different CY types (LS-CY: light-sensitive chrome yellow $PbCr_{1-x}S_xO_4$, with $x \approx 0.5$; LF-CY: lightfast chrome yellow monoclinic $PbCrO_4$; CO: chrome orange $(1-x)PbCrO_4{\cdot}x\,PbO$); V and RL indicate spots containing also vermilion and red lead (see Figure 2A), while the white circle indicates the location where only red lead was identified. Triangles and Roman numerals show the regions of FTIR analyses (see Figure 2B).

edge structure (μ-XANES) and μ-XRF to obtain microscale spatially resolved speciation of the chromium oxidation state. Experimental details are given in the Supporting Information together with a detailed summary of the analytical results (Table S1).

The MA-XRF maps of the painting (Figure 1B,C) show that Pb and Cr are the main elemental constituents of the sunflower petals, the orange corollas, and the table area. In the pale-yellow background, Zn is the predominant element (Figure 1B), thus suggesting the presence of zinc white (ZnO), while Pb and Cr are present in significantly lower quantities. In some of the ochre and orange tones of the sunflower petals, Hg and/or Cu and As were found in addition to Pb and Cr (Figure 1C), arising from the presence of vermilion (HgS) and/or emerald green ($3\,Cu(AsO_2)_2{\cdot}Cu(CH_3COO)_2$). In areas of the sunflower petals and the upper region of the vase with no or very little Pb and Cr, Fe is the main constituent element instead, thus indicating the use of a yellow ochre (iron hydroxide based pigment). All the above-mentioned pigments are frequently encountered in works by Van Gogh.[5] In the green(ish) areas, Pb and Cr are sometimes found together, in addition to Cu and As, thus suggesting the use of mixtures or overlapping brush strokes of emerald green and CYs. The Pb-L_α/Cr-K_α XRF intensity ratio changes throughout the painting (Figure 1B), thus suggesting a distribution of different CY types. However, the presence of other Pb- and/or Cr-based pigments also frequently used by Van Gogh, such as red lead (Pb_3O_4), lead white ($PbCO_3$/$Pb_3(CO_3)_2(OH)_2$), or viridian ($Cr_2O_3{\cdot}2\,H_2O$),[5] and variations of the paint thickness (giving rise to self-absorption of variable magnitude), could also cause a change in the Pb-L_α/Cr-K_α intensity ratio. No meaningful S-distribution maps could be recorded, mainly because of the spectral overlap between the S-K and Pb-M XRF signals and the limited MA-XRF sensitivity for these signals.

More reliable insights into the distribution of the different types of CY were obtained by performing vibrational spectroscopic and structural analyses at a select number of points on the surface of the *Sunflowers* painting (Figures 1D and 2) and on two microsamples (Table S1).

As visible in the standard reference spectra (Figure 2A; gray lines) and consistent with previous studies,[8,15] the presence of the characteristic sulfate symmetric stretching mode ($\nu_1(SO_4^{2-})$, 976 cm^{-1}) combined with the broadening and the wavenumber shift toward higher values for both the chromate symmetric stretching band ($\nu_1(CrO_4^{2-})$, from 841 to 844 cm^{-1}) and the chromate bending signals ($\nu_4(CrO_4^{2-})$, from 400 to 407 cm^{-1}) allowed the distinction to be made between the LS-CY ($x \approx 0.5$) and the LF-CY (i.e., monoclinic $PbCrO_4$). In the reflection mid-FTIR profiles (Figures 2B and 3D; gray lines), typical spectral features for the identification of the LS-CY ($x \approx 0.5$) are the inverted sulfate asymmetric stretching band ($\nu_3(SO_4^{2-})$) and the two sulfate bending signals ($\nu_4(SO_4^{2-})$), whose shape and wavenumber position differ from those of other sulfate-based compounds.[8,16] The inverted chromate asymmetric stretching band ($\nu_3(CrO_4^{2-})$) of LS-CY is broader than that of LF-CY.

In the light-yellow table area, noninvasive Raman (Figures 1D and 2A; points 1 and 2) and reflection mid-FTIR analyses (Figure 2B; spectrum I) revealed the presence of LS-CY ($x \approx 0.5$). This finding was confirmed by SR-based μ-XRD and vibrational spectroscopic analysis of a sample from the region (F458/4), in which a few grains of cerussite ($PbCO_3$) were also identified (Figure S1). In the zinc-rich pale-yellow background, the Raman spectrum (Figures 1D and 2A; point 3) again demonstrated the presence of LS-CY ($x \approx 0.5$). In the corresponding FTIR spectrum (Figure 2B; spectrum III), only zinc white (inverted ν(Zn–O) band below 520 cm^{-1}), zinc oxalate (1364, 1320 cm^{-1}) and zinc carboxylate (1540, 1465, 1398, 744, 718 cm^{-1}) were identified. The latter two represent reaction products of ZnO with the oil binder.[17,18]

For the sunflower petals, various CYs appear to have been used. In the light-yellow areas, a type of LS-CY ($x \approx 0.5$) very similar to that detected in the table and background was identified by Raman spectroscopy (Figures 1D and 2A; points 4–8). On the other hand, in the ochre-yellow petals, Raman spectra from five different areas (points 9–13) highlight the presence of LF-CY. In two locations, Raman (points 14–15) and FTIR data (Figure 2B; spectrum II) show that LF-

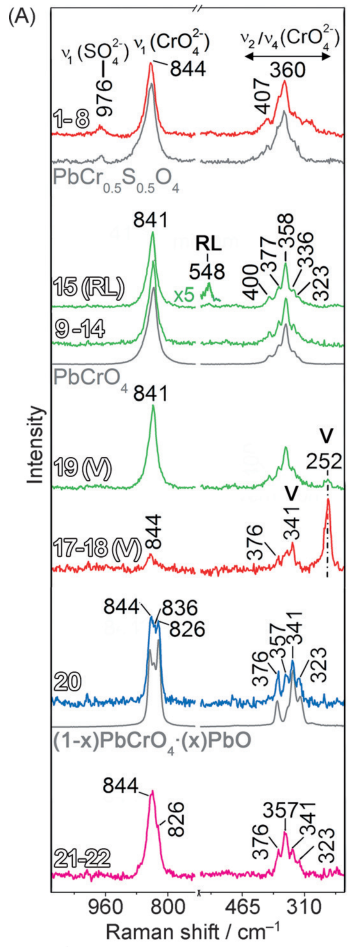

Figure 2. Noninvasive (A) Raman and (B) reflection mid-FTIR spectra collected from the locations indicated in Figure 1 D and from the corresponding reference compounds (gray lines). In (A), selection of the spectral profiles acquired from different areas of the painting (1–8: pale-yellow background/light-yellow petals/light-yellow table; 9–14/15(RL): ochre-yellow petals; 17–18(V)/19(V): ochre petals; 20: orange corolla; 21–22: orange-yellow petals). V and RL denote the spots where chrome yellow is mixed with vermilion or red lead; the color of the spectrum indicates the type of chrome yellow (red: LS-CY; green: LF-CY; blue: CO; magenta: LS-CY + CO).

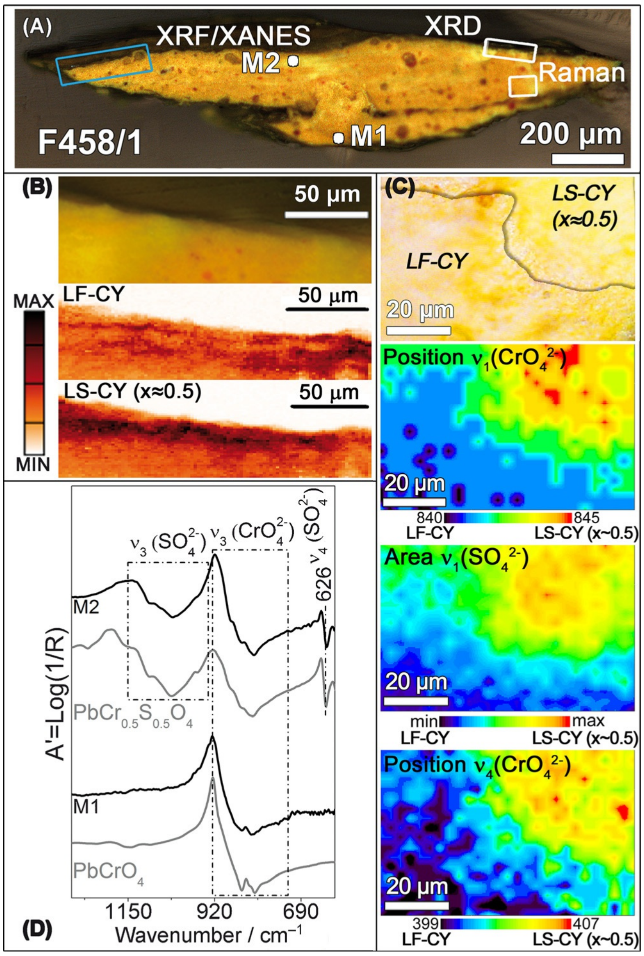

Figure 3. A) Photomicrograph of sample F458/1 and LF-CY and LS-CY ($x \approx 0.5$) distribution maps obtained by B) SR μ-XRD (map size: 190×51 μm^2; pixel size ($h \times v$): 2×1 μm^2) and C) μ-Raman (map size: 78×51 μm^2; step size: 3×3 μm^2) (see Figure S2 for a selection of the corresponding XRD and Raman profiles). D) Reflection μ-FTIR spectra obtained from a yellow-orange tone (M1) and a light-yellow area (M2) of the sample, compared to those of reference compounds (gray lines). In (A) white rectangles and labels indicate the positions where data of (B–D) were collected. Cyan rectangle shows the area of Figure S3A where μ-XRF/μ-XANES analyses were performed.

CY is mixed with LS-CY ($x \approx 0.5$) or red lead (Raman signal at 548 cm^{-1}).[19] The latter compound was also identified as the main component of a red protrusion (point 16; spectrum not shown).

SR-based μ-XRD and μ-Raman mapping experiments of regions of interest of sample F458/1 (Figure 3 A–C) confirmed the noninvasive findings, and also provided further insights into the spatial distribution of the two CY types: LF-CY is the chief constituent of the yellow-orange shades, while LS-CY ($x \approx 0.5$) is the main phase in the light-yellow hues.

In the XRD maps (see Figure 3 B and Figure S2A in the Supporting Information), the distribution of these two types of CY is indicated by the different position of the main diffractions signals (e.g., (111) and (020) peaks) that progressively shift towards higher scattering vector values with increasing sulfur content.[8,15] In the Raman maps (see Figure 3 C and Figure S2B), the localization of the LS-CY ($x \approx 0.5$), which corresponds to the light-yellow hues, is visible as an increase of the area of the $\nu_1(SO_4^{2-})$ band (976 cm^{-1}) and a wavenumber shift toward higher values for the $\nu_1(CrO_4^{2-})$ and $\nu_4(CrO_4^{2-})$ modes (from 841 to 844 cm^{-1} and from 400 to 407 cm^{-1}, respectively). Reflection μ-FTIR spectroscopic investigations (Figure 3 D) confirm the identification of LS-CY ($x \approx 0.5$; spectrum M2) and LF-CY (M1).

Raman spectroscopy performed in three different spots of the ochre petals (Figures 1 D and 2 A; points 17–19) showed either LS-CY ($x \approx 0.5$) or LF-CY to be present, mixed with vermilion (signals at 252, 341 cm^{-1}).[19]

Chrome orange ($(1-x)PbCrO_4\cdot(x)PbO$) (here denoted as CO) was detected in an orange corolla (Figures 1 D and 2 A, point 20; see also the spectrum of the corresponding reference compound). In two regions of the sunflower petals with an orange-yellow tone (points 21–22), this compound is present in a mixture with LS-CY ($x \approx 0.5$).

Since the three identified types of lead chromate based compounds are used in mixture with other pigments, as well as alone, the visual assessment of any color change because of chromate photoreduction is not straightforward. The degradation state of the chrome yellow paint was therefore evaluated by determining the Cr speciation state via SR-based μ-XANES/μ-XRF analysis at the Cr K-edge of samples F458/4 (Figure 4; light-yellow table area) and F458/1 (Figure S3; upper-right ochre-yellow petal).

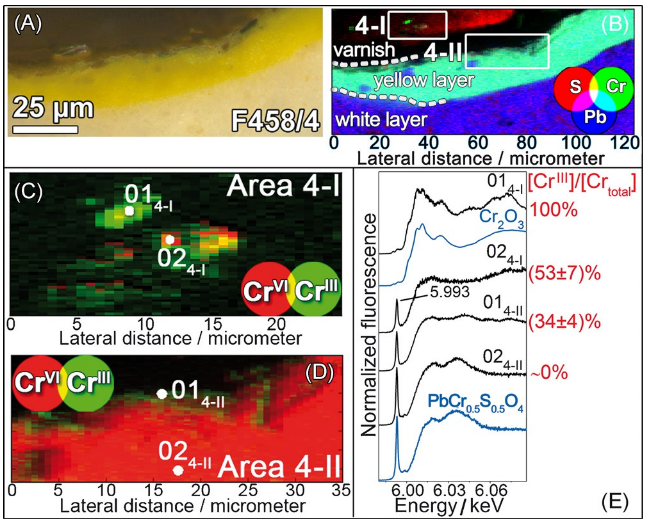

Figure 4. A) Photomicrograph detail of sample F458/4 where SR μ-XRF/μ-XANES analyses were performed (see Figure S1 for a photo of the entire sample). B) RGB composite SR μ-XRF images of S/Cr/Pb (map size: $124\times51.2\ \mu m^2$; pixel size ($h\times v$): $1\times0.25\ \mu m^2$; energy: 6.090 keV). C, D) RG composite Cr^{VI}/Cr^{III} chemical state maps (pixel size ($h\times v$): $0.7\times0.2\ \mu m^2$) and (E) μ-XANES spectra collected from areas indicated in (C, D). Maps (C, D) were acquired in the regions shown in (B).

In the Cr K-edge μ-XANES spectra, the intensity decrease of the pre-edge peak at 5.993 keV (electronic transition 1s→3d) as well as the shift of the absorption edge toward lower energies are clear indications of the local presence of reduced Cr (e.g., Cr^{III} and Cr^{V}).[11,20] The relative abundance of the latter species was obtained by linear combination fitting of unknown XANES spectra against sets of profiles of reference materials, comprising a series of Cr^{III} compounds and a Cr^{V} compound (sodium bis(2-hydroxy-2-methylbutyrato)oxochromate(V)). Similar to earlier investigations,[20] the best description of the μ-XANES data from the paint samples is obtained when the spectra of Cr^{III} oxides and either Cr^{III} sulfates or organo Cr^{III} compounds (i.e., Cr^{III} acetate hydroxide or Cr^{III} acetylacetonate) are included in the fitting model together with that of LF-CY/LS-CY (Table S2). For this reason, the relative amount of reduced Cr is subsequently expressed as $[Cr^{III}]/[Cr_{total}]$.

Clear indications for the gradual conversion of Cr^{VI} to Cr^{III} were found inside the varnish layer of sample F458/4. At one location, a chromium-rich particle (Figure 4C; area 4-I) appears to be completely reduced to the Cr^{III} state and the corresponding μ-XANES spectrum (Figure 4E; point $01_{4\text{-}I}$) resembles that of Cr_2O_3. In the area surrounding this particle, the relative abundance of Cr^{III} was estimated to be around 50% (point $02_{4\text{-}I}$).

Even more revealing is that in another region, the chemical state maps (Figure 4D; area 4-II) clearly show that Cr^{III} species are present as a 2–3 μm thick layer right at the varnish/paint interface. Here, the relative abundance of Cr^{III} is around 35%, while it decreases to 0% when going deeper inside the yellow paint (Figure 4E; points $01_{4\text{-}II}$–$02_{4\text{-}II}$). This pattern is very similar to that previously observed in photochemically aged LS-CY ($x > 0.4$) paint models.[9–11]

The Cr speciation results are consistent with the non-invasive reflection mid-FTIR data obtained from a region close to the sampling spot (Figure 2B; spectrum I): the inverted broad band at 465 cm^{-1} strongly resembles that present in the spectrum of a photoaged $PbCr_{0.5}S_{0.5}O_4$ paint and previously assigned to Cr^{III} oxide compounds.[9,21] The presence of Cr^{III} compounds could also be demonstrated at the surface of sample F458/1 (Figure S3).

Since a significant color alteration can be observed in artificially aged LS-CY models, caused by a thin degradation layer containing Cr^{III} compounds,[9–11] we infer that in the *Sunflowers* painting, at least at the two sampled spots, a color change arising from CY reduction has occurred. In the areas of the painting where LS-CY is present (see Figure 1D), we consider it likely that a similar darkening has taken place.

In summary, the noninvasive identification and macro-scale level distribution of the light-sensitive chrome yellow has allowed us to identify selected locations of the painting with the highest probability/risk of color change because of Cr^{VI} reduction and that call for careful monitoring over time. Further investigations are underway to extend our knowledge on the composition of additional yellow areas of the painting. Moreover, we have provided evidence that in two areas of the painting, the chrome yellow pigments have degraded through $Cr^{VI}\rightarrow Cr^{III}$ reduction, as earlier observed in other works by Van Gogh.[22–24]

Since the chrome yellows were often encountered in mixtures with other pigments (red lead, vermilion, zinc white, emerald green), further research is required to distinguish between the deliberate color contrasts obtained by Van Gogh by using specific paint mixtures and the subsequent effects of darkening by pigment degradation. Ongoing research aims to explore how these added pigments (most of them with well-known photoredox properties) and possibly the corresponding degradation compounds[25–28] may influence the stability of lead chromates and contribute to visible color change. The findings of this study, supported by those of earlier works,[9,11] will allow the elaboration of a more accurate, safe and controlled strategy for the light exposure of the painting.

Acknowledgements

We acknowledge financial support from the Italian MIUR project SICH-PRIN (2010329WPF_001) and BELSPO (Brussels) Project S2-ART (SD04A), GOA "SOLARPAINT" (Research Fund Antwerp University, BOF-2015), and FWO (Brussels) projects G.0C12.13, G.0704.08, G.01769.09. We thank ESRF (EC-1051, HG-26) and DESY (I-20120312 EC) for beamtime grants received. Noninvasive analysis of *Sunflowers* were supported by the EU FP7 programme CHARISMA (Grant 228330) and the Fund Inbev-Baillet Latour (Brussels). L.M. acknowledges financial support from the CNR Short Term Mobility Programme-2013. We thank Muriel Geldof, Luc Megens, Suzan de Groot (The Netherlands Cultural Heritage Agency, RCE), Chiara Grazia, David Buti (CNR-ISTM and SMAArt Centre), and the staff of the Van Gogh Museum for their collaboration.

Keywords: dyes/pigments · lead chromate · photoreduction · vibrational spectroscopy · X-ray absorption spectroscopy

How to cite: *Angew. Chem. Int. Ed.* **2015**, *54*, 13923–13927
Angew. Chem. **2015**, *127*, 14129–14133

[1] a) http://vangoghletters.org/vg/, Letter 668 (accessed August 2015); b) http://vangoghletters.org/vg/, Letters 593, 595, 684, 687, 710, 863 (accessed August 2015).
[2] M. Bailey, *The Sunflowers are mine: The story of Van Gogh's masterpiece*, Frances Lincoln, London, **2013**.
[3] L. Van Tilborgh, E. Hendriks, *Van Gogh Museum Journal* **2001**, 17–44.
[4] H. Kühn, M. Curran, in *Artists' Pigments. A Handbook of Their History and Characteristics*, *Vol. 1* (Ed.: L. Feller), Cambridge University Press, London **1986**, pp. 187–204.
[5] M. Geldof, L. Megens, J. Salvant in *Van Gogh's Studio Practice* (Eds.: M. Vellekoop, M. Geldof, E. Hendriks, L. Jansen, A. de Tagle), Yale University Press, New Haven and London, **2013**, pp. 238–256.
[6] K. H. Lister, C. Peres, I. Fiedler in *Van Gogh and Gauguin: The Studio of the South* (Eds.: D. W. Druick, P. K. Zegers), Thames & Hudson, London, **2001**, pp. 354–369.
[7] E. Rathbone, W. H. Robinson, E. Steele, M. Steele, *Van Gogh Repetitions*, Yale University Press, New Haven and London, **2013**.
[8] L. Monico, K. Janssens, C. Miliani, B. G. Brunetti, M. Vagnini, F. Vanmeert, G. Falkenberg, A. Abakumov, Y. Lu, H. Tian, J. Verbeeck, M. Radepont, M. Cotte, E. Hendriks, M. Geldof, L. Van der Loeff, J. Salvant, M. Menu, *Anal. Chem.* **2013**, *85*, 851–859.
[9] L. Monico, K. Janssens, C. Miliani, G. Van der Snickt, B. G. Brunetti, M. Cestelli Guidi, M. Radepont, M. Cotte, *Anal. Chem.* **2013**, *85*, 860–867.
[10] L. Monico, G. Van der Snickt, K. Janssens, W. De Nolf, C. Miliani, J. Verbeeck, H. Tian, H. Tan, J. Dik, M. Radepont, M. Cotte, *Anal. Chem.* **2011**, *83*, 1214–1223.
[11] L. Monico, K. Janssens, M. Cotte, A. Romani, L. Sorace, C. Grazia, B. G. Brunetti, C. Miliani, *J. Anal. At. Spectrom.* **2015**, *30*, 1500–1510.
[12] H. Tan, H. Tian, J. Verbeeck, L. Monico, K. Janssens, G. Van Tendeloo, *Angew. Chem. Int. Ed.* **2013**, *52*, 11360–11363; *Angew. Chem.* **2013**, *125*, 11570–11573.
[13] M. Alfeld, J. Vaz Pedroso, M. Van Eikema Hommes, G. Van der Snickt, G. Tauber, J. Blaas, M. Haschke, K. Erler, J. Dik, K. Janssens, *J. Anal. At. Spectrom.* **2013**, *28*, 760–767.
[14] C. Miliani, F. Rosi, B. G. Brunetti, A. Sgamellotti, *Acc. Chem. Res.* **2010**, *43*, 728–738.
[15] L. Monico, K. Janssens, E. Hendriks, B. G. Brunetti, C. Miliani, *J. Raman Spectrosc.* **2014**, *45*, 1034–1045.
[16] C. Miliani, F. Rosi, A. Daveri, B. G. Brunetti, *Appl. Phys. A* **2012**, *106*, 295–307.
[17] J. Hermans, K. Keune, A. Van Loon, P. Iedema, *J. Anal. At. Spectrom.* **2015**, *30*, 1600–1608.
[18] J. Van der Weerd, M. Geldof, L. Van der Loeff, R. M. A. Heeren, J. J. Boon, *Kunsttechnol. Konserv.* **2003**, *17*, 407–416.
[19] L. Burgio, R. J. Clark, *Spectrochim. Acta Part A* **2001**, *57*, 1491–1521.
[20] L. Monico, K. Janssens, M. Cotte, L. Sorace, F. Vanmeert, B. G. Brunetti, C. Miliani, *Microchem. J.* **2016**, *124*, 272–282.
[21] S. Musić, M. Malijković, S. Popović, *Croat. Chem. Acta* **1999**, *72*, 789–802.
[22] L. Monico, G. Van der Snickt, K. Janssens, W. De Nolf, C. Miliani, J. Dik, M. Radepont, E. Hendriks, M. Geldof, M. Cotte, *Anal. Chem.* **2011**, *83*, 1224–1231.
[23] L. Monico, K. Janssens, M. Alfeld, M. Cotte, F. Vanmeert, C. G. Ryan, G. Falkenberg, D. L. Howard, B. G. Brunetti, C. Miliani, *J. Anal. At. Spectrom.* **2015**, *30*, 613–626.
[24] L. Monico, K. Janssens, F. Vanmeert, M. Cotte, B. G. Brunetti, G. Van der Snickt, M. Leeuwestein, J. Salvant Plisson, M. Menu, C. Miliani, *Anal. Chem.* **2014**, *86*, 10804–10811.
[25] W. Anaf, K. Janssens, K. De Wael, *Angew. Chem. Int. Ed.* **2013**, *52*, 12568–12571; *Angew. Chem.* **2013**, *125*, 12800–12803.
[26] F. Vanmeert, G. Van der Snickt, K. Janssens, *Angew. Chem. Int. Ed.* **2015**, *54*, 3607–3610; *Angew. Chem.* **2015**, *127*, 3678–3681.
[27] C. Clementi, F. Rosi, A. Romani, R. Vivani, B. G. Brunetti, C. Miliani, *Appl. Spectrosc.* **2012**, *66*, 1233–1241.
[28] K. Keune, J. J. Boon, R. Boitelle, Y. Shimadzu, *Stud. Conserv.* **2013**, *58*, 199–210.

Received: June 25, 2015
Revised: September 16, 2015
Published online: October 20, 2015

